

On the Correlation between the Negative Intrinsic Viscosity and the Rotatory Relaxation Time of Solvent Molecules in Dilute Polymer Solutions

Takenao Yoshizaki, Yoshio Takaeda, and Hiromi Yamakawa*

Department of Polymer Chemistry, Kyoto University, Kyoto 606-01, Japan

Received August 6, 1993; Revised Manuscript Received September 25, 1993*

ABSTRACT: The rotatory relaxation time $\tau_{r,0}$ of solvent molecules in dilute polymer solutions was determined from dynamic depolarized light scattering measurements. The solutions examined are those of polyisobutylene (dimer) in benzene at 25.0 °C (Θ) and of poly(dimethylsiloxane) in bromocyclohexane at 29.5 °C (Θ), the intrinsic viscosity of their oligomers with very small molecular weights being known to become negative. It is found that $\tau_{r,0}$ of benzene is independent of the mass concentration c of the solute, while $\tau_{r,0}$ of bromocyclohexane decreases with increasing c , indicating that Lodge's view of the negative intrinsic viscosity is not always valid. A discussion is given of a possible source of this breakdown of his view and of the procedure of determining the intrinsic viscosity that is to be compared with the theoretical value evaluated within the framework of classical hydrodynamics.

Introduction

Recently, Lodge and his co-workers^{1,2} made a series of well-designed experimental studies of the mean rotatory relaxation time $\tau_{r,0}$ of solvent molecules in dilute polymer solutions to examine possible effects of the addition of solute polymers to the solvent. The purpose of these investigations was indeed to elucidate the physical process that the observed infinitely high-frequency intrinsic viscosity, $[\eta]_{\infty, \text{obs}}$, becomes negative in some cases.⁴ Thus they showed that $\tau_{r,0}$ decreases with increasing solute concentration for solutions of flexible polymers such as poly(1,4-butadiene)¹ and polyisoprene⁵ in Aroclor 1248 (A1248), both with negative $[\eta]_{\infty, \text{obs}}$.⁴ These results have led them to the new and rather astonishing view that $[\eta]_{\infty, \text{obs}}$ includes not only a *direct* (intrinsic) contribution $[\eta]_{\infty}$ associated with the solute polymer chain itself but also an *indirect* one from a change in an *effective* solvent viscosity, and it may possibly become negative if this viscosity decreases with increasing solute concentration. In the present paper, we examine experimentally whether the above view is valid in the case of other solvents, since A1248 is rather a special solvent used only for viscoelastic measurements.

In order to clarify the point, it is pertinent to review here in more detail Lodge's phenomenological explanation of the negative $[\eta]_{\infty, \text{obs}}$ with the effective solvent viscosity.^{1,2} They first introduced the effective solvent viscosity $\eta_0(c)$, which depends on the mass concentration c of the solute, defined by

$$\eta_0(c) = \eta_0 \tau_{r,0} / \tau_{r,0}^0 \quad (1)$$

where $\eta_0 = \eta_0(0)$ is the viscosity of the pure solvent and $\tau_{r,0}^0$ is the value of $\tau_{r,0}$ at $c = 0$. The dependence of $\eta_0(c)$ on c arises from that of $\tau_{r,0}$ on c , so that, at small c , $\eta_0(c)$ may be written in the form

$$\tau_{r,0} \propto \eta_0(c) = \eta_0(1 + kc + \dots) \quad (2)$$

where k is a coefficient independent of c . Then they assumed that the solute molecules are regarded as hydrodynamic resisters in a continuous *solvent* with the viscosity coefficient $\eta_0(c)$, so that the solution viscosity η

(at a given frequency) may be written in the form

$$\eta = \eta_0(c)(1 + [\eta]c + \dots) \quad (3)$$

with $[\eta]$ the conventional intrinsic viscosity (at that frequency). Note that this $[\eta]$ is the intrinsic quantity for the solute molecule that is determined from the usual viscosity measurements if $\eta_0(c)$ does not depend on c and that is to be compared with the theoretical value evaluated within the framework of classical hydrodynamics. Thus the solute molecules make direct and indirect contributions to η through $[\eta]$ and $\eta_0(c)$, respectively. The observed intrinsic viscosity $[\eta]_{\text{obs}}$ is then defined as usual by

$$\eta = \eta_0(1 + [\eta]_{\text{obs}}c + \dots) \quad (4)$$

From eqs 2-4, we have

$$[\eta]_{\text{obs}} = [\eta] + k \quad (5)$$

Note that eqs 1-5 are equivalent to eqs 11, 21, and 22 of ref 2. Since the addition of the hydrodynamic resisters to a viscous fluid necessarily gives rise to excess nonnegative energy dissipation, $[\eta]$ must be nonnegative at any frequency. Necessarily, therefore, it follows from eqs 2 and 5 that $\tau_{r,0}$ must decrease with increasing c (for small c), i.e., $k < 0$, if $[\eta]_{\infty, \text{obs}}$ is negative.

Now the quantity $[\eta]_{\infty}$ arises from the excess energy dissipation due to small parts of a polymer chain and is closely related to the (zero-frequency) intrinsic viscosity $[\eta]$ of its oligomer with very small molecular weight, so that $[\eta]_{\text{obs}}$ is negative for the oligomer if $[\eta]_{\infty, \text{obs}}$ is negative, and vice versa. We have recently found that $[\eta]_{\text{obs}}$ becomes negative for oligomer samples of polyisobutylene (PIB) in benzene at 25.0 °C (Θ)⁶ and for those of poly(dimethylsiloxane) (PDMS) in bromocyclohexane at 29.5 °C (Θ).⁷ According to the above deduction, for these solvents $\tau_{r,0}$ must then decrease with increasing c . We examine this by determining $\tau_{r,0}$ as a function of c for benzene and bromocyclohexane in the respective solutions above from dynamic depolarized light scattering (LS) measurements.

We note that fortunately these two solute-solvent systems are quite suitable for the present purpose. The optical anisotropies of PIB and PDMS are very small compared to those of benzene and bromocyclohexane, respectively, and therefore the spectra of the depolarized component of the light scattered by the solvent molecules may be determined rather accurately.

* Abstract published in *Advance ACS Abstracts*, November 1, 1993.

Table I. Values of M_w , x_w , and M_w/M_n for Isobutylene Oligomer and Oligo- and Poly(dimethylsiloxane)s

sample	code	M_w	x_w	M_w/M_n
PIB	OIB2	1.12×10^2	2	1.00
PDMS	ODMS2 ^a	2.37×10^2	2	1.00
	PDMS1 ^b	8.26×10^3	110	1.05

^a M_w of ODMS2 had been determined by ¹H NMR spectroscopy.⁸^b M_w of PDMS1 had been determined from LS measurements in toluene at 25.0 °C.⁷

Experimental Section

Materials. One PIB sample and two PDMS samples used in this work are the same as those used in the previous studies.⁶⁻⁸ The PIB sample is the isobutylene dimer that is a mixture of 2,4,4-trimethyl-1-pentene (Aldrich Chemical Co.; purity > 99%) and 2,4,4-trimethyl-2-pentene (Aldrich Chemical Co.; purity > 98%) in the molar (or weight) ratio of 96:4.⁶ One of the PDMS samples is a fraction separated by fractional distillation under reduced pressure from the commercial sample supplied by Toshiba Silicone Co., Ltd., named Low Boil Fractions, and the other is a fraction separated by fractional precipitation from the sample TSF451-500 of the same source.⁸ The values of the weight-average molecular weight M_w , the weight-average degree of polymerization x_w , and the ratio of M_w to the number-average molecular weight M_n are listed in Table I.

A polystyrene (PS) sample, F80, used for the determination of the (relative) transmittance of a Fabry-Perot (FP) interferometer is the same as that used in the previous study of the transport factors ρ and Φ for long flexible polymers,⁹ which had been obtained by reprecipitation from the standard sample F-80 supplied by Tosoh Co., Ltd.

The solvent benzene used for dynamic depolarized LS measurements was purified according to a standard procedure, and the solvent bromocyclohexane (Tokyo Kasei Kogyo Co.; 98% purity) used for the same measurements was purified by distillation under reduced pressure in a dry nitrogen atmosphere after dehydration with sodium carbonate anhydride. The solvent methyl ethyl ketone (MEK) used for the determination of the transmittance of the FP interferometer was purified according to a standard procedure.

Dynamic Depolarized Light Scattering. (i) **Apparatus and Measurements.** The photometer used for all dynamic depolarized LS measurements is the same as that used in the previous study of the mean-square optical anisotropy,¹⁰ i.e., a Brookhaven Instruments Model BI-200SM goniometer with a minor modification of its light source part and with a detector alignment newly assembled to incorporate the FP interferometer in it, whose detailed description was given in the previous paper.¹⁰ Thus we here describe its outline and the method of triple passes with the single FP interferometer¹¹ adopted in the present study.

Vertically polarized light of wavelength 488 nm from a Spectra-Physics Model 2020 argon ion laser equipped with a Model 583 temperature-stabilized etalon for single-frequency-mode operation was used as a light source. It was made highly vertically (v) polarized by passing through a Glan-Thompson (GT) prism with an extinction ratio smaller than 10^{-5} . The scattered light was measured at a scattering angle of 90°. Its horizontal (H) component, i.e., the depolarized (Hv) component, which was extracted from the total scattered light intensity by the use of the same GT prism as above, was analyzed with a Burleigh Instruments Model RC-110 FP interferometer equipped with a Model RC-670 pair of plane mirrors with a flatness of $\lambda/200$ and a reflectivity of 97.5%. The intensity of the Hv component filtered through the FP interferometer was measured by an EMI 9893B/350 photomultiplier tube.

Before proceeding to give a further description, it is convenient to give here a brief explanation of the transmittance of the FP interferometer. For the light of angular frequency ω , in the ideal case its transmittance $T(\omega)$ may be given by¹¹

$$T(\omega) = T_{\max} [1 + (2F/\pi)^2 \sin^2(\pi\omega/\delta)]^{-1} \quad (6)$$

where T_{\max} is the maximum transmittance, F is a parameter representing the resolution of the FP interferometer, and δ is the

free spectral range (FSR) given by

$$\delta = \pi c_0/d \quad (7)$$

with c_0 the velocity of light in the atmosphere and d the distance between the mirrors composing the interferometer. As seen from eq 6, $T(\omega)$ is a periodic function with period δ . The quantities T_{\max} and F depend on the quality of the mirrors (and also on the adjustment of the interferometer). Although the functional form of $T(\omega)$ really deviates from its ideal one given by eq 6, the small deviation is immaterial for the present explanation. In general, the value of F is much larger than unity, so that $T(\omega)$ may be written as a sum of the Lorentzians as

$$T(\omega) \simeq \sum_{j=0}^{\infty} T_j(\omega) \quad (8)$$

with

$$T_j(\omega) = T_{\max} [1 + (2F/\delta)^2(\omega - j\delta)^2]^{-1} \quad (9)$$

It is seen from this expression that the parameter F is equal to the finesse as defined as the ratio of FSR to a full width at half-maximum of the peak.

In the case of the triple passing, a light beam is passed through the single pair of the mirrors three times by the use of two retroreflectors (right angle prisms) placed in the front and rear of the pair of mirrors, so that the interferometer becomes equivalent to an alignment of the three identical (original) interferometers. In this case, $T_j(\omega)$ in eq 8 may be given by

$$T_j(\omega) = T_{\max}^3 [1 + (2F/\delta)^2(\omega - j\delta)^2]^{-3} \quad (10)$$

(Note that F is then not equal to the finesse.) From a comparison of eq 9 with eq 10, it is seen that every peak of the transmittance becomes sharp by use of the triple passing. In this work, we used a Burleigh Instruments Model RC-22 pair of retroreflectors for this method.

Now consider the scattered light which has the (true) power spectrum $I(\omega_0 + \Delta\omega)$ as a function of the angular frequency $\omega_0 + \Delta\omega$, with ω_0 being that of the incident light. The observed (apparent) intensity I_{ap} of the light after passing through the interferometer with $T(\omega)$ given by eq 8 with eq 10 may then be written in the form

$$I_{\text{ap}} = \int_{-\omega_0}^{\infty} T(\omega_0 + \Delta\omega) I(\omega_0 + \Delta\omega) d(\Delta\omega) \quad (11)$$

In general, $I(\omega_0 + \Delta\omega)$ may be considered to decrease rapidly to zero with increasing $|\Delta\omega|$, so that we may put

$$I(\omega_0 + \Delta\omega) = 0 \quad \text{for } |\Delta\omega| > (n - 1/2)\delta \quad (12)$$

with n a positive integer properly chosen. Then we have

$$I_{\text{ap}} = \sum_{j=j_0-n+1}^{j_0+n-1} \int_{-(n-1/2)\delta}^{(n-1/2)\delta} T_j(\omega_0 + \Delta\omega) I(\omega_0 + \Delta\omega) d(\Delta\omega) \quad (13)$$

where j_0 is the integer that satisfies the inequality

$$|\omega_0/\delta - j_0| < 1/2 \quad (14)$$

From eq 10 (or eq 9), we obtain the relation

$$T_j(\omega_0 + \Delta\omega) = T_{j-j_0}(\Delta\omega - \Delta\omega_{\text{ap}}) \quad (15)$$

with

$$\Delta\omega_{\text{ap}} = j_0\delta - \omega_0 \quad (16)$$

Equation 13 may then be reduced to

$$I_{\text{ap}}(\Delta\omega_{\text{ap}}) = \sum_{j=-n+1}^{n-1} \int_{-(n-1/2)\delta}^{(n-1/2)\delta} T_j(\Delta\omega - \Delta\omega_{\text{ap}}) I(\Delta\omega) d(\Delta\omega) \quad (17)$$

where $I(\Delta\omega) = I(\omega_0 + \Delta\omega)$, and the argument of I_{ap} has been explicitly shown.

It is seen from eq 17 that we may determine T_j by measuring I_{ap} with a line (or extremely sharp) spectrum for $I(\Delta\omega)$. In practice, following Ouano and Pecora,¹² we determined it by measuring the polarized component of the light scattered from

a solution of the PS sample F80 ($M_w = 7.32 \times 10^5$) in MEK at $c \approx 1 \times 10^{-3}$ g/cm³ and at 25.0 or 29.5 °C.

The FSR (δ) was determined to be 1.43×10^{13} rad/s (corresponding to 75.7 cm⁻¹) for the present setting of d , using the sodium doublet of separation 0.597 nm at 589.3 nm (in vacuum).

The most concentrated solution of each sample was prepared gravimetrically and made homogeneous by continuous stirring for ca. 10 min at room temperature for the samples OIB2 and ODMS2 and for ca. 10 h at 50 °C for the sample PDMS1. These solutions and the solvents were optically purified by filtration through a Teflon membrane of pore size 0.1 or 0.45 μ m. The solutions of lower concentrations were obtained by successive dilution. The weight concentrations of the test solutions were converted to the solute mass concentrations c (in g/cm³) by the use of the densities of the solutions.

Before and after each measurement on the solution or solvent, the transmittance of the FP interferometer was determined in the manner as described above. (We note that the Hv component scattered from pure benzene was not measured since the absolute intensity of the spectrum was not necessary.) In the present measurements with the triple passing, the finesse could be kept at 60–65 during a single measurement, which took ca. 40 min.

(ii) **Determination of the Depolarized Spectrum.** If the FSR is chosen to be sufficiently larger than the width of the (true) spectrum $I(\Delta\omega)$, we may put $n = 1$ in eq 12, and therefore $I(\Delta\omega)$ may then be determined from eq 17 with $n = 1$, i.e., the integral equation,

$$I_{ap}(\Delta\omega_{ap}) = \int_{-\delta/2}^{\delta/2} K(\Delta\omega - \Delta\omega_{ap}) I(\Delta\omega) d(\Delta\omega) \quad (18)$$

In the present case of the triple passing, the kernel K is equal to the T_0 given by eq 10 (in the ideal case). Although the actual transmittance is somewhat different from this T_0 in form, the difference was found to be negligibly small (see below). Thus we assumed for the kernel K

$$K(\Delta\omega) = T_{\max}^3 [1 + (2F/\delta)^2 (\Delta\omega)^2]^{-3} \quad (19)$$

and determined the parameters T_{\max} and F so that the squared difference between the observed transmittance and the one calculated from eq 19 might be minimized.

In the case of the single passing, for which the kernel K is equal to the T_0 given by eq 9, the integral equation (18) may be solved analytically. Unfortunately, however, eq 18 with eq 19 cannot be solved analytically. Thus we solved it numerically as follows. We first express the (true) spectrum I as a sum of a constant term and several normalized Lorentzians, i.e.,

$$I(\Delta\omega) = A_0 + \sum_{i=1}^m (A_i c_i / \pi) [1 + (c_i \Delta\omega)^2]^{-1} \quad (20)$$

and then determine the coefficients $(A_0, A_1, \dots, A_m) = \{A_{m+1}\}$ and $(c_1, c_2, \dots, c_m) = \{c_m\}$ so that the sum f of residual errors defined by

$$f(\{A_{m+1}\}, \{c_m\}) = \sum_{i=1}^N |I_{ap,i} - I_{ap}(\Delta\omega_i)|^2 \quad (21)$$

may be minimized, where $I_{ap,i}$ is the (apparent) intensity observed at $\Delta\omega_{ap} = \Delta\omega_i$ and $I_{ap}(\Delta\omega_i)$ is the (apparent) intensity calculated from eq 18 with eqs 19 and 20. We note that each Lorentzian in eq 20 thus determined has no physical meaning.

In Figure 1 are shown apparent and true FP spectra of the Hv component for pure benzene at 25.0 °C. The unfilled circles represent the values of the apparent (observed) Hv component $I_{Hv,ap}$, and the solid curve represents the values of the true one I_{Hv} evaluated numerically, where the latter values have been scaled so that the maximum of I_{Hv} may be equal to that of $I_{Hv,ap}$. (Note that I_{Hv} and $I_{Hv,ap}$ have different dimensions.) In the figure, values of the kernel K appearing in eq 18 (or the transmittance of the FP interferometer) are also plotted against $\Delta\omega$. The filled circles represent its observed values, and the dashed curve represents the best-fit values calculated from eq 19, with the optimum values of T_{\max} and F determined as mentioned above. The agreement between the observed and calculated values of K is very good, and therefore the adoption of the functional form given by eq 19 for K may be considered to cause no serious error in the evaluation

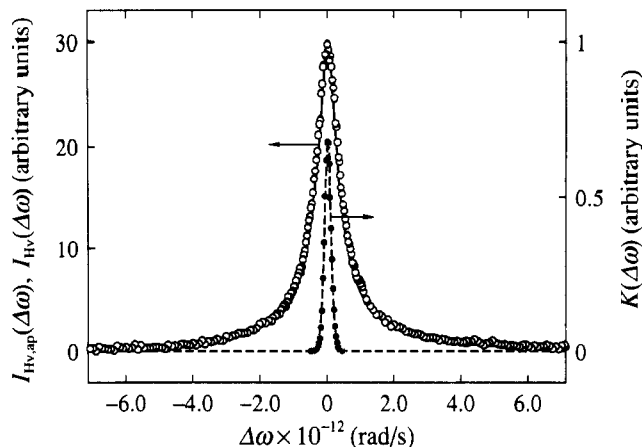


Figure 1. Plots of $I_{Hv,ap}(\Delta\omega)$ and $I_{Hv}(\Delta\omega)$ for benzene at 25.0 °C and $K(\Delta\omega)$ against $\Delta\omega$. The unfilled circles and solid curve represent the values of $I_{Hv,ap}$ and I_{Hv} , respectively, and the filled circles and dashed curve present the observed and best-fit values of K , respectively.

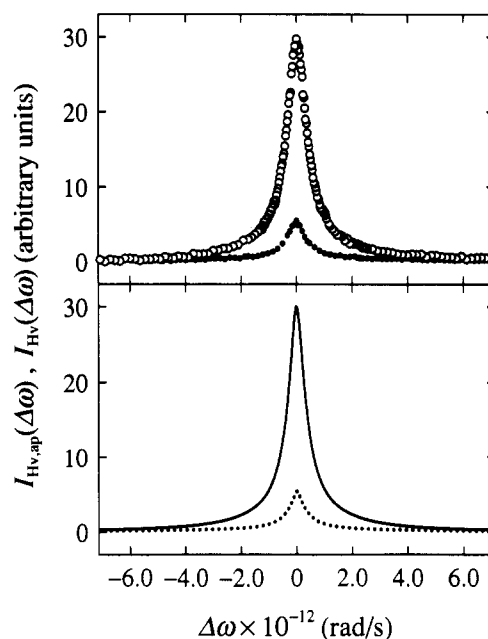


Figure 2. Plots of $I_{Hv,ap}(\Delta\omega)$ and $I_{Hv}(\Delta\omega)$ against $\Delta\omega$ for benzene and OIB2 at 25.0 °C. The unfilled and filled circles represent the values of $I_{Hv,ap}$ for benzene and OIB2, respectively, and the solid and dotted curves represent the values of I_{Hv} for benzene and OIB2, respectively.

of the true spectrum. In general, the quantity f defined by eq 21 depends on the number m of the basis functions; it is a monotonically decreasing function of m . In this case of pure benzene, it was found to be actually independent of m for $m \geq 10$, and thus the values represented by the solid curve are those evaluated with $m = 10$. For other spectra, we also put $m = 10$, for convenience. It is seen from the figure that the true spectrum is sharper, although slightly, than the apparent one.

Results

In Figure 2 are shown apparent and true FP spectra of the Hv component for pure benzene and the neat sample OIB2 at 25.0 °C. The unfilled and filled circles represent the values of the apparent component $I_{Hv,ap}$ for benzene and OIB2, respectively, and the solid and dotted curves represent the values of the true one I_{Hv} for benzene and OIB2, respectively. Figure 3 shows similar plots for bromocyclohexane (unfilled circles and solid curve) and the neat samples ODMS2 and PDMS1 (filled circles and dotted curves) at 29.5 °C. We note that $I_{Hv,ap}$ could be determined for the neat samples OIB2, ODMS2, and

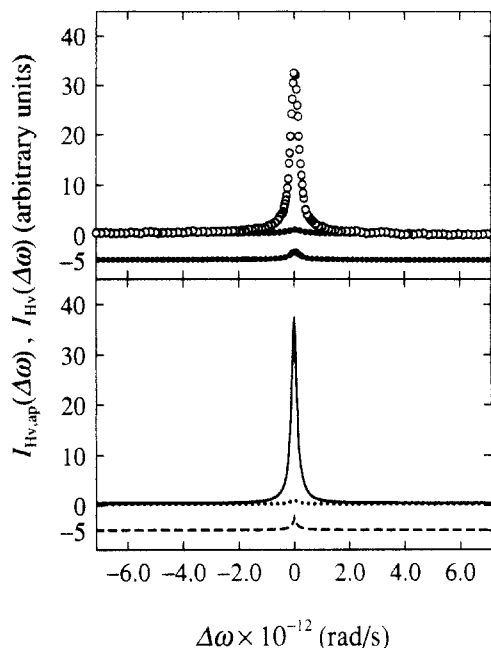


Figure 3. Plots of $I_{Hv,ap}(\Delta\omega)$ and $I_{Hv}(\Delta\omega)$ against $\Delta\omega$ for bromocyclohexane, ODMS2, and PDMS1 at 29.5 °C. The unfilled circles represent the values of $I_{Hv,ap}$ for bromocyclohexane, and the filled circles represent those for ODMS1 and PDMS1, the points for PDMS1 being shifted downward by 5. The solid curve represents the values of I_{Hv} for bromocyclohexane, and the dotted curves represent those for ODMS2 and PDMS1, the curve for PDMS1 being shifted downward by 5.

PDMS1 but not for a neat PIB sample with high molecular weight since the former three are liquids but the latter is not so. It is seen from the figures that the optical anisotropies of the solutes PIB and PDMS are extremely small compared to those of the solvents benzene and bromocyclohexane, respectively. It is also seen that the FSR (1.43×10^{13} rad/s) was set sufficiently large compared to the width of the spectrum of the Hv component in all cases, so that the true spectrum could be determined from eq 18.

The "excess" Hv component $\Delta I_{Hv,solv}(\Delta\omega)$ due to solvent molecules may be calculated from

$$\Delta I_{Hv,solv}(\Delta\omega) = I_{Hv,soln}(\Delta\omega) - \phi_{solute} I_{Hv,solute}(\Delta\omega) \quad (22)$$

where $I_{Hv,soln}$ and $I_{Hv,solute}$ are the Hv components for the solution and neat solute, respectively, and ϕ_{solute} is the volume fraction of the latter. Figure 4 shows plots of $\Delta I_{Hv,solv}$ against $\Delta\omega$ for benzene in the solution of OIB2 at 25.0 °C. The solid and dotted curves represent the values at $c = 0.389$ and 0 (pure benzene) g/cm³, respectively, where the latter has been scaled so that its maximum may be equal to that of the former. They are seen to be very close to each other. Figures 5 and 6 show similar plots for bromocyclohexane in the solutions of ODMS2 and PDMS1 at 29.5 °C, respectively, at $c = 0.359$ and 0 g/cm³ for the former and at $c = 0.331$ and 0 g/cm³ for the latter. The spectrum is seen to become appreciably broader for the solution than for the pure solvent in the case of PDMS in bromocyclohexane, in contrast to the case of PIB in benzene.

Now, according to Keyes and Kivelson,¹³ the depolarized component of the light scattered from a pure solvent may be given by

$$I_{Hv,solv}(\Delta\omega) \propto [1 + (\bar{\tau}_{r,0}\Delta\omega)^2]^{-1} \quad (23)$$

where $\bar{\tau}_{r,0}$ is the apparent rotatory relaxation time and is proportional to the true relaxation time $\tau_{r,0}$ as defined as

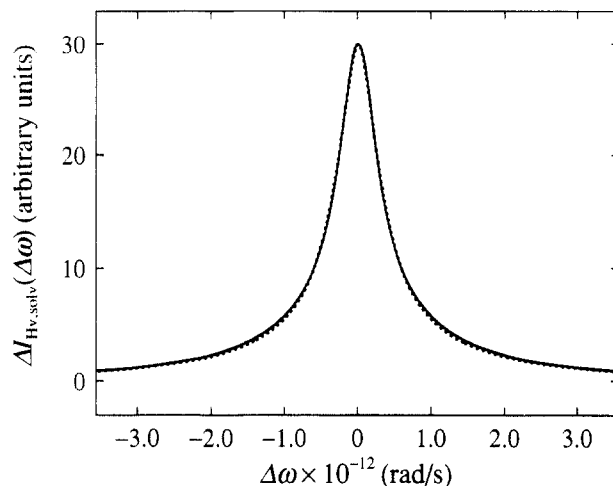


Figure 4. Plots of $\Delta I_{Hv,solv}(\Delta\omega)$ against $\Delta\omega$ for benzene in the solution of OIB2 at 25.0 °C. The solid and dotted curves represent the values at $c = 0.389$ and 0 (pure benzene) g/cm³, respectively.

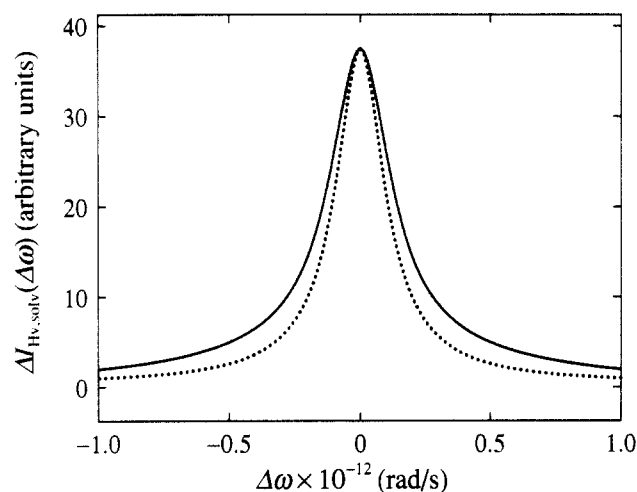


Figure 5. Plots of $\Delta I_{Hv,solv}(\Delta\omega)$ against $\Delta\omega$ for bromocyclohexane in the solution of ODMS2 at 29.5 °C. The solid and dotted curves represent the values at $c = 0.359$ and 0 (pure bromocyclohexane) g/cm³, respectively.

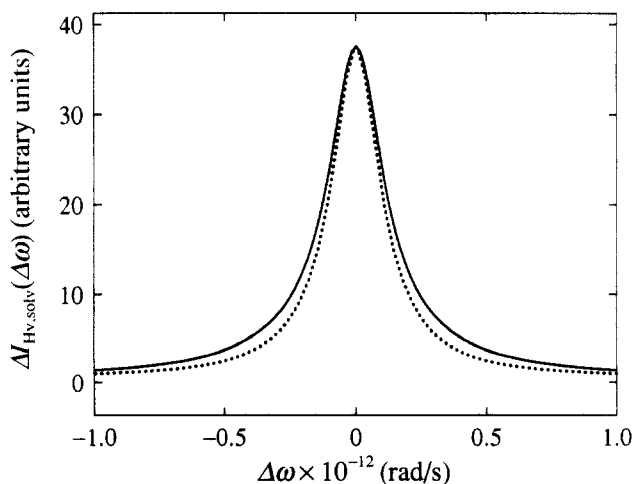


Figure 6. Plots of $\Delta I_{Hv,solv}(\Delta\omega)$ against $\Delta\omega$ for bromocyclohexane in the solution of PDMS1 at 29.5 °C. The solid and dotted curves represent the values at $c = 0.331$ and 0 (pure bromocyclohexane) g/cm³, respectively.

$1/6D_{r,0}$, with $D_{r,0}$ the rotatory diffusion coefficient of the solvent molecules, i.e.,

$$\bar{\tau}_{r,0} = C\tau_{r,0} \quad (24)$$

The proportionality constant C is, in general, dependent

Table II. Values of the Half-Width at Half-Maximum (hwhm) of the Excess Depolarized Spectra and $\tau_{r,0}$ for Benzene and Bromocyclohexane

$c, \text{g/cm}^3$	$10^{-12} \text{ hwhm, rad/s}$	$\tau_{r,0}, \text{ps}$
OIB2/Benzene (25.0 °C)		
0	0.39 ₁	2.5 ₆
0.110	0.38 ₆	2.5 ₉
0.179	0.38 ₇	2.5 ₈
0.242	0.39 ₀	2.5 ₆
0.389	0.38 ₁	2.6 ₃
0.534	0.38 ₉	2.5 ₇
ODMS2/Bromocyclohexane (29.5 °C)		
0	0.11 ₅	8.6 ₉
0.136	0.12 ₆	8.0 ₀
0.233	0.14 ₀	7.1 ₆
0.359	0.15 ₄	6.4 ₉
0.475	0.12 ₉	7.7 ₃
PDMS1/Bromocyclohexane (29.5 °C)		
0	0.11 ₅	8.6 ₉
0.110	0.11 ₇	8.5 ₂
0.161	0.12 ₂	8.2 ₂
0.292	0.12 ₅	7.9 ₈
0.331	0.13 ₈	7.2 ₆

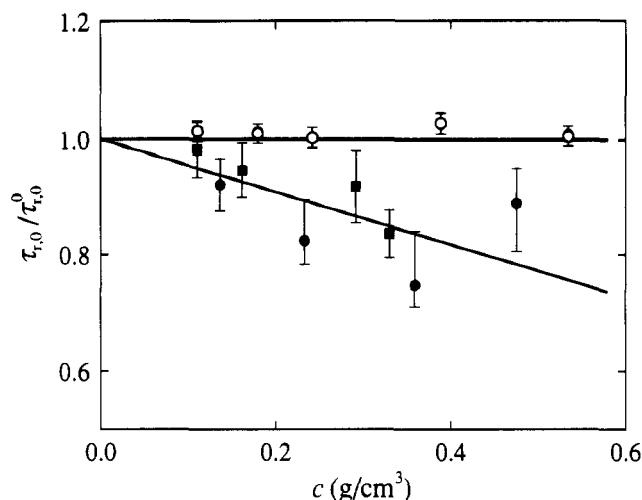
on the static and dynamic orientational correlations between the solvent molecules,¹³ but its explicit expression is not necessary for the present discussion. From eq 23, $\tau_{r,0}$ is seen to be equal to the reciprocal of the half-width at half-maximum (hwhm) of the depolarized spectrum, and, indeed, $\tau_{r,0}$ has often been evaluated in this way.^{14,15} Thus, in this paper, we evaluate $\tau_{r,0}$ for solvent molecules not only in pure solvents but also in solutions from hwhm. (Strictly, the depolarized spectrum cannot be reproduced by a single Lorentzian. For example, the spectrum in Figure 1 for benzene is nearly composed of three Lorentzians).

In Table II are given the values of hwhm determined from the depolarized spectra and those of $\tau_{r,0}$ thus evaluated, for benzene molecules in the solutions of PIB at 25.0 °C and for bromocyclohexane molecules in the solutions of PDMS at 29.5 °C, both at various concentrations c . The value 2.5₆ ps of $\tau_{r,0}$ obtained for pure benzene is rather in good agreement with the values 2.85 and 2.7 ps obtained for benzene at 25.0 °C by Alms et al.¹⁴ and by Patterson and Griffiths,¹⁵ respectively, where the former value has been calculated from the original value 2.91 ps obtained at 23.6 °C, using the relation between $\tau_{r,0}$ and the temperature reported by Patterson and Griffiths.¹⁵ It is seen that $\tau_{r,0}$ is independent of c for benzene, while it decreases with increasing c for bromocyclohexane.

Discussion

Rotatory Relaxation Time. Although $\tau_{r,0}$ determined in the last section cannot, in general, be equated exactly to $\tau_{r,0}$ because of the factor C in eq 24, Patterson and Griffiths¹⁵ have shown that the orientational correlations between the solvent molecules, which lead to its introduction, have only small or no effects on the depolarized spectrum as far as pure benzene is concerned. We may therefore assume that C is equal to unity for benzene molecules in dilute solutions. As for bromocyclohexane, although there is no available information about the effect of this orientational correlation, it may possibly arise from dipole-dipole interactions between bromocyclohexane molecules as in the case of chloroform.¹⁴ However, we are here mainly concerned with the concentration dependence of $\tau_{r,0}$ and therefore simply equate it to $\tau_{r,0}$ also for bromocyclohexane. A possible effect caused by the change in C with concentration is discussed below.

Now, Figure 7 shows plots of the ratio $\tau_{r,0}/\tau_{r,0}^0 (= \tau_{r,0}/\tau_{r,0}^0)$ of $\tau_{r,0}$ to its value $\tau_{r,0}^0$ in the pure solvent against c .

**Figure 7.** Plots of $\tau_{r,0}/\tau_{r,0}^0$ against c : (O) for benzene in the solution of OIB2 at 25.0 °C; (●) for bromocyclohexane in the solution of ODMS2 at 29.5 °C; (■) for bromocyclohexane in the solution of PDMS1 at 29.5 °C.

The unfilled circles represent the values for benzene in the solutions of OIB2 at 25.0 °C, and the filled circles and squares represent those for bromocyclohexane in the solutions of ODMS2 and PDMS1, respectively, at 29.5 °C. The vertical line segments attached to the data points indicate the limit of experimental error. The results for the solutions of ODMS2 and PDMS1 are seen to agree with each other within experimental error, and therefore $\tau_{r,0}$ may be expected to be independent of M_w also for PIB. In contradiction to Lodge's view mentioned in the Introduction, $\tau_{r,0}/\tau_{r,0}^0$ is independent of c for benzene in the solutions of OIB2 within experimental error despite the fact that its $[\eta]$ in benzene is negative.⁶ On the other hand, the decrease in $\tau_{r,0}/\tau_{r,0}^0$ with increasing c for bromocyclohexane supports this view (if C is independent of c).

This conclusion for bromocyclohexane, which has been derived on the assumption that C is independent of c , requires some remarks. If C is greater than unity for it as in the case of chloroform investigated by Patterson and Griffiths¹⁵ and if C decreases with increasing c , the decrease in $\tau_{r,0}$ may be ascribed to that in C . Even if this is the case, Lodge's view seems still valid for bromocyclohexane. The reason for this is that the decrease in C leads to that in $\tau_{r,0}$ since the decrease in C may be regarded as arising from the fact that the added solute molecules weaken the orientational correlations between solvent molecules.

At any rate, the present experimental results demonstrate that his view, which has been deduced from experimental data for solutions of several flexible polymers in A1248, is not always valid but restricted to the case of certain solvents (like A1248) having strong intermolecular interactions. It is evident that this breakdown arises from his explanation of the negative intrinsic viscosity mentioned in the Introduction, i.e., the replacement of the solvent viscosity η_0 with the phenomenological effective solvent viscosity $\eta_0(c)$ defined by eq 1, which has no theoretical foundation, as stated by himself.²

Determination of $[\eta]$ from $[\eta]_{\text{obs}}$. Although we have written down eq 5 in the context of Lodge's view, we may rather regard it as an equation defining the quantity k in terms of the observed intrinsic viscosity $[\eta]_{\text{obs}}$ and the intrinsic quantity $[\eta]$ for the solute molecule that is to be compared with the theoretical value evaluated within the framework of classical hydrodynamics. Indeed, we ourselves already determined $[\eta]$ and k separately by the use

of an equation equivalent to eq 5 in the previous studies of $[\eta]$ for PIB⁶ and PDMS,⁷ in which the symbol η^* was used in place of k and it was estimated from an analysis of the dependence of $[\eta]_{\text{obs}}$ on the molecular weight on the basis of the helical wormlike chain theory,^{16,17} regarding it as an adjustable parameter. Thus the parameter k (or η^*) introduced in our empirical procedure is formally equivalent to Lodge's k but different from the latter in physical meaning, which is determined from the dependence of $\tau_{r,0}$ on c . We note that, if k is positive, it cannot be determined unambiguously from experiments in our procedure since the positive k may be treated as an increase in the hydrodynamic diameter of the beads composing the model chain, so that we have considered only the case of negative k .

In the procedure of Lodge, $[\eta]$ is estimated from $[\eta]_{\text{obs}}$ and k by the use of eq 5 with eq 2. As shown in the last subsection, however, this procedure gives the incorrect result that $[\eta]_{\text{obs}} = [\eta] > 0$ ($k = 0$) for the solution of PIB in benzene. Then there arises a question of whether it may give indeed correct results for $[\eta]$ for solutions of flexible polymers in A1248. Thus it seems inadequate to compare values of $[\eta']_{\infty} (= [\eta']_{\infty, \text{obs}} - k)$ estimated by Lodge and his co-workers^{1,2} for these solutions with theoretical values¹⁸ predicted by the polymer dynamics based on classical hydrodynamics, as done by them.

Conclusion

On the basis of the present experimental results for the rotatory relaxation time $\tau_{r,0}$ for the solvents benzene and bromocyclohexane in the solutions of polyisobutylene and poly(dimethylsiloxane), respectively, it has been shown that Lodge's view of the negative intrinsic viscosity is not always valid. It is evident that its breakdown is due to his two assumptions that $\tau_{r,0}$ is proportional to the effective solvent viscosity $\eta_0(c)$ and that η is expressed in terms of $\eta_0(c)$ and $[\eta]$. Our empirical procedure of determining $[\eta]$ from the observed intrinsic viscosity $[\eta]_{\text{obs}}$ as previously⁶

proposed seems more reliable for practical use. For a thorough understanding of the negative intrinsic viscosity, we must develop a theory, starting from a completely microscopic formulation of the solution viscosity, since the problem cannot be treated within the framework of classical hydrodynamics.

Acknowledgment. This research was supported in part by a Grant-in-Aid (04650809) from the Ministry of Education, Science, and Culture, Japan.

References and Notes

- (1) Morris, R. L.; Amelar, S.; Lodge, T. P. *J. Chem. Phys.* **1988**, *89*, 6523.
- (2) Lodge, T. P. *J. Phys. Chem.* **1993**, *97*, 1480 and also papers cited therein.
- (3) Ferry, J. D. *Viscoelastic Properties of Polymers*, 3rd ed.; Wiley: New York, 1980; Chapter 9.
- (4) Man, V. F. Ph.D. Thesis, University of Wisconsin, Madison, WI, 1984. Merchak, P. A. Ph.D. Thesis, University of Wisconsin, Madison, WI, 1987.
- (5) Amelar, S.; Krahn, J. R.; Hermann, K. C.; Morris, R. L.; Lodge, T. P. *Spectrochim. Acta Rev.* **1991**, *14*, 379.
- (6) Abe, F.; Einaga, Y.; Yamakawa, H. *Macromolecules* **1991**, *24*, 4423.
- (7) Yamada, T.; Koyama, H.; Yoshizaki, T.; Einaga, Y.; Yamakawa, H. *Macromolecules* **1993**, *26*, 2566.
- (8) Yamada, T.; Yoshizaki, T.; Yamakawa, H. *Macromolecules* **1992**, *25*, 1487.
- (9) Konishi, T.; Yoshizaki, T.; Yamakawa, H. *Macromolecules* **1991**, *24*, 5614.
- (10) Takaeda, Y.; Yoshizaki, T.; Yamakawa, H. *Macromolecules* **1993**, *26*, 3742.
- (11) Hernandez, G. *Fabry-Perot Interferometers*; Cambridge University Press: Cambridge, U.K., 1986.
- (12) Ouano, A. C.; Pecora, R. *Macromolecules* **1980**, *13*, 1167.
- (13) Keyes, T.; Kivelson, D. *J. Chem. Phys.* **1972**, *56*, 1057.
- (14) Alms, G. R.; Bauer, D. R.; Brauman, J. I.; Pecora, R. *J. Chem. Phys.* **1973**, *58*, 5570.
- (15) Patterson, G. D.; Griffiths, J. E. *J. Chem. Phys.* **1975**, *63*, 2406.
- (16) Yamakawa, H. *Annu. Rev. Phys. Chem.* **1984**, *35*, 23.
- (17) Yoshizaki, T.; Nitta, I.; Yamakawa, H. *Macromolecules* **1988**, *21*, 165.
- (18) Yoshizaki, T.; Yamakawa, H. *J. Chem. Phys.* **1988**, *88*, 1313.